RSC Advances

ROYAL SOCIETY OF CHEMISTRY

www.rsc.org/advances

Graphical Abstract

Effect of alkali and alkaline earth metal ions on benzyl alcohol oxidation activity of titanate nanotubes-supported Au catalysts

Devadutta Nepak and D. Srinivas*

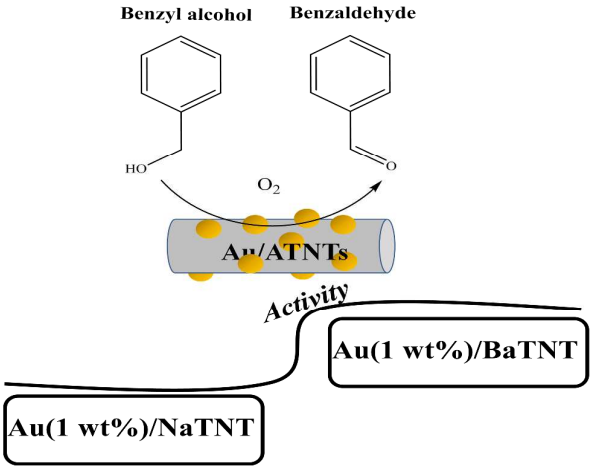

Au suppored on barium titanate nanotubes showed higher catalytic activity for selective oxidation of benzyl alcohol with molecular oxygen.

Journal Name

RSCPublishing

ARTICLE

Effect of alkali and alkaline earth metal ions on benzyl alcohol oxidation activity of titanate nanotubes-supported Au catalysts

Devadutta Nepak[a,b] and Darbha Srinivas*[a,b]

Cite this: DOI: 10.1039/x0xx00000x

Received 00th April 2015,
Accepted 00th April 2015

DOI: 10.1039/x0xx00000x

www.rsc.org/

Sodium titanate nanotubes (NaTNT) were prepared by alkali treatment of anatase titania. They were then ion-exchanged with alkali and alkaline earth metal ions to get ATNT (A = Li^+, K^+, Cs^+, Mg^{2+}, Ca^{2+}, $Sr^{2+}$and Ba^{2+}). Gold (1 – 5 wt%) was supported on these nanotubes by deposition-precipitation method and investigated as a catalyst for selective oxidation of benzyl alcohol with air/molecular oxygen (1 atm) under solvent- and alkali-free conditions. Detailed characterization by X-ray powder diffraction, high resolution transmission electron microscopy, N_2-physisorption, diffuse reflectance UV-visible spectroscopy, X-ray photoelectron spectroscopy and CO_2-temperature-programmed desorption techniques revealed that basicity of the catalyst influences the uptake, mean particle size, electronic property and oxidation activity of the supported gold. Benzaldehyde formed with a selectivity of about 99%. Catalytic activity (turnover frequency) was found to have a direct relation with basicity and inverse relation with the Au particle size. Among the catalysts investigated, Au/BaTNT having higher basicity, smaller Au particles and higher metal dispersion showed enhanced catalytic activity than the other Au/ATNT catalysts. Pd addition to Au leading to Au-Pd/BaTNT increased the activity (TOF) but lowered the selectivity for benzaldehyde (80 wt%). Titanate nanotubes donate electron density to Au particles, yielding electron rich Au ions, which are responsible for activating molecular oxygen and oxidizing benzyl alcohol. Au/BaTNT having higher basicity and lower size Au nanoparticles than the other Au/ATNT activates molecular oxygen more easily and thereby, enhances the catalytic activity.

Introduction

Heterogeneous catalysis by gold is now a well fascinating research topic. Previously it was ignored for a long time as bulk gold is chemically inert. The field of catalysis by nano-gold was provoked by two contemporaneous discoveries made by Hutchings[1] and Haruta[2] for acetylene hydrochlorination and low-temperature CO oxidation, respectively. This led to several other explorations and exploitations of nano-gold and gold containing catalysts in oxidation, epoxidation, direct synthesis of hydrogen peroxide, hydrogenation, coupling and water-gas shift reactions through green chemistry practices.[3] In particular, selective liquid-phase oxidation of alcohols to corresponding carbonyl compounds using gold catalysts under moderate conditions is highly desirable from economic and environmental perspectives.[3, 4]

The catalytic performance of supported gold nanoparticles (Au NPs) can be altered by controlling the particle size of Au, by choosing the right kind of support and by building strong contact of gold with the support (through metal–support peripheral interface or via charge transfer from the support to gold).[5] The effect of strong metal–support interactions (SMSI) was first observed in TiO_2-supported noble metal systems reported by Tauster et al[5] in 1978. One of the early hypotheses for this effect was that the alteration of the charge state of the metal by electron transfer from or to a support leads to an improvement in the ability to activate reactants and thereby influencing the catalytic properties of the metal.[6] This hypothesis was confirmed experimentally by several researchers. Bruix et al[7] successfully interpreted the enhanced activity of platinum particles supported on ceria in water–gas shift reaction as the "electronic metal–support interaction" (EMSI), a term that was recently coined by Campbell.[8] However, intrinsic metal effects, such as the electronic quantum size effect[9] and the structure–sensitivity geometrical effect[10] should be ruled out for a complete understanding of the EMSI effect. For supported metal particle/cluster catalysts, a complete elimination of the intrinsic metal effects is particularly difficult or even impossible. Milone et al.[11] reported that the catalytic properties of supported gold catalysts strongly depend on the type and structure of the support. From the comparative study of Fe_2O_3-, ZnO-, CaO-, and Al_2O_3-supported gold catalysts, they found that the basicity and lattice oxygen of support have significant effects on the catalytic performance.

Recently, the 1-D nanoscale alkali titanates have attracted much interest in heterogeneous catalysis as catalyst supports. In particular, after the simple alkaline hydrothermal synthesis, sodium titanate nanotubes (NaTNT) reported for the first time by Kasuga et al[12] have emerged as promising functional material. The NaTNT have well-defined mesopores with a wall thickness of a few nanometers. They expose a large proportion of the Na^+ counterions on the inner and outer surfaces of the nanotubes. These Na^+ ions are ion-exchangeable.[13] Ion-exchange has been established as an effective method for preparing highly dispersed supported metal catalysts with a narrow metal particle size distribution for use in heterogeneous catalysis.[14] Moreover, the semiconducting properties of titanate nanotubes may lead to strong electronic interaction between the support and metal, which could improve catalytic performance in redox reactions. Specifically, titanate nanotubes have been used as catalyst support for platinum catalyzed cyclohexene hydrogenation-dehydrogenation,[15] iridium and cobalt catalyzed water splitting for hydrogen production,[16] gold catalyzed water-gas shift reaction[17] and CO oxidation[18,19] and bimetallic gold-palladium catalyzed direct synthesis of hydrogen peroxide.[20] Recently, we have reported the application of Au and Au-Pd supported on NaTNT for oxidation of primary and secondary alcohols.[21] In continuation to this work, we report here a study of Au supported on various alkali and alkaline earth metal ion-exchanged titanate nanotubes for benzyl alcohol oxidation. The influence of basicity of the support on the physicochemical characteristics and catalytic activity of gold is investigated.

Experimental

Catalyst preparation

Titanium dioxide (98% anatase TiO_2), sodium hydroxide (NaOH), and alkali and alkaline earth metal nitrates were obtained from Thomas Baker Chemicals Ltd. Chloroauric acid ($HAuCl_4.3H_2O$) was purchased from HiMedia Chemicals Ltd. and palladium acetate ($Pd(OAc)_2$) was procured from Aldrich Co. All reagents were used as received and without any further purification.

NaTNT was prepared as reported by us earlier.[21] To synthesize ion-exchanged titanate nanotubes, ATNT (A = Li^+, K^+, Cs^+, Mg^{2+}, Ca^{2+}, Sr^{2+} and Ba^{2+}), 2.5 g of dried NaTNT was suspended in 120 mL of 1.0 M aqueous solution of alkali and alkaline earth metal nitrates. The suspension was stirred for 8 h while maintaining the temperature at 80 °C. The solid was separated and the ion-exchange procedure was repeated for another two times. The solid isolated was washed with deionized water, filtered and dried at 110 °C overnight to obtain ATNT. In the case of Cs^+, Sr^{2+} and Ba^{2+} exchanged materials the concentration of the nitrate solution used was 0.5 M instead of 1.0 M, as solubility is an issue with these salts.

In the preparation of 1, 3 and 5 wt.% Au supported on ATNT, an appropriate amount of 2 mM aqueous solution of $HAuCl_4.3H_2O$ was added drop-wise to 1 g of ATNT suspended in 100 mL of deionized water. The suspension was stirred vigorously for 12 h while maintaining the temperature at 80 °C. All this operation was done in dark or by covering the contents with an aluminium foil. The solid obtained was filtered, washed with deionized water and dried at 110 °C for 20 h to obtain the gold loaded ATNT. The materials were then reduced in flowing hydrogen (20 mL/min) at 250 °C for 2 h to yield the final catalysts.

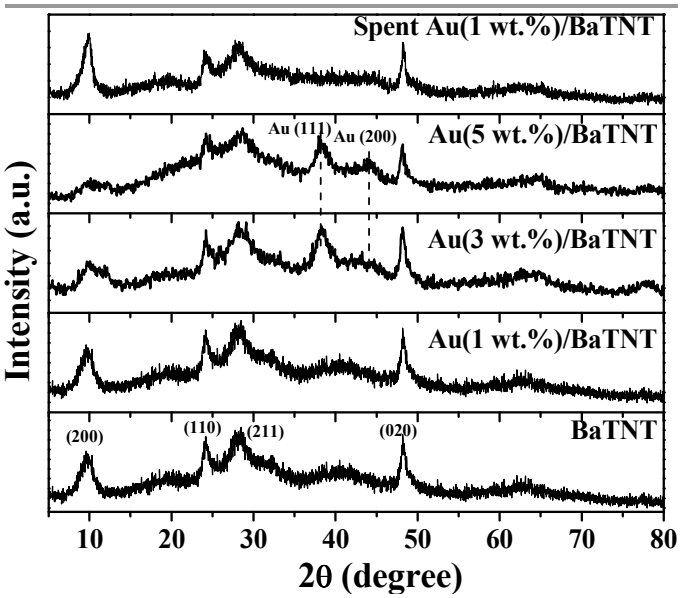

Figure 1. XRD patterns of BaTNT and Au/BaTNT.

Au-Pd(2 wt%, 1:1)/BaTNT was prepared in the same manner as described above by adding simultaneously, required amounts of aqueous $HAuCl_4.3H_2O$ (2 mM) and $Pd(OAc)_2$ (2 mM) solutions to a BaTNT suspension.

Catalyst characterization techniques

The metal loadings were determined by Inductively coupled plasma-optical emission spectroscopy (ICP-OES; Spectro Arcos). Au/ATNTs were digested in aqua-regia. Standard solutions of known concentrations were used for calibration. X-ray powder diffraction (XRD) patterns of the catalyst samples were recorded immediately after reduction in H_2 flow (250 °C, 2 h) on a Philips X'Pert Pro diffractometer using Cu-Kα radiation (λ = 0.15406 nm) and a proportional counter detector with a scanning angle (2θ) of 5–80° at a scan speed of 4° min^{-1}. High resolution transmission electron microscopic images (HRTEM) were taken on a FEI Technai-F30 instrument with a 300 kV field emission gun. Specific surface area, pore volume and pore diameter of the catalysts were determined from N_2 adsorption–desorption isotherms measured at -196 °C using a Quantachrome, USA (Autosorb-1C) equipment. Prior to N_2 adsorption, the samples were evacuated at 200 °C for 2 h. A reference alumina sample (supplied by Quantachrome, USA) was used to calibrate the instrument. Diffuse reflectance UV-visible (DRUV-vis) spectroscopic measurements of the powder samples were performed on a Shimadzu UV-2550 spectrophotometer equipped with an integrating sphere attachment (ISR 2200); $BaSO_4$ was used as the standard. Temperature-programmed desorption (TPD) studies were carried out on a Micromeritics Auto Chem 2910 instrument using CO_2 as probe molecule to quantify the amount of basic sites. In a typical experiment, 0.1 g of the catalyst was taken in a U-shaped, flow-through, quartz sample tube. Prior to measurements, the catalyst was pre-treated in He (30 mL/min) at 250 °C for 1 h. It was then cooled to 25 °C and a mixture of CO_2 in He (10 vol%) was fed to the sample (30 mL/min) for 1 h. Then, the sample was flushed with He (30 mL/min) for 1 h at 100 °C. Before starting the desorption analysis, baseline was checked for stability. The CO_2-TPD measurements were carried

Journal Name

RSCPublishing

ARTICLE

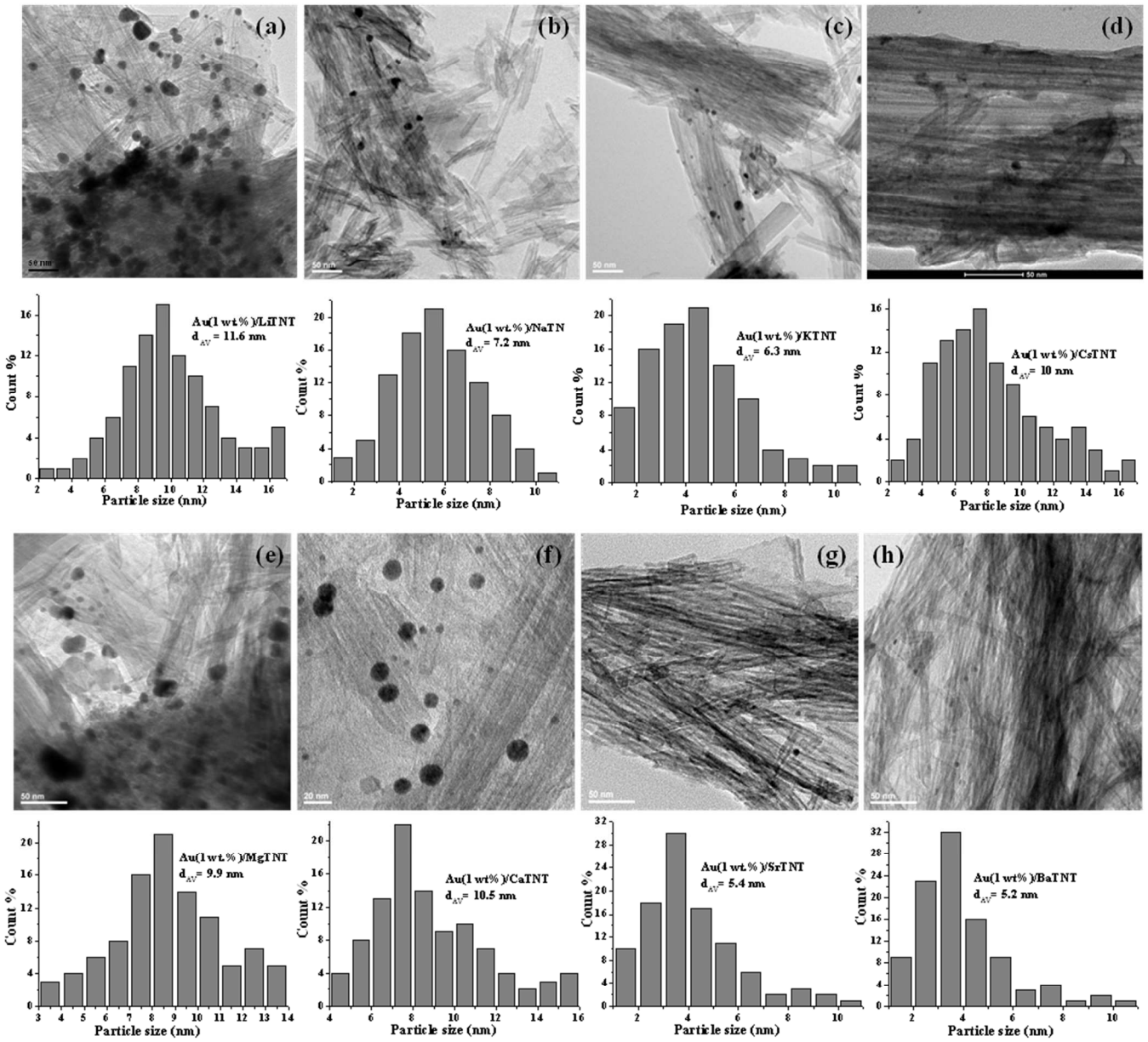

Figure 2. HRTEM images and particle size distribution histograms of Au(1 wt%)/ATNT catalysts

out in the temperature range of 100 – 500 °C. The area of the desorption peaks gave the amount of basic sites present in the catalyst. X-ray photoelectron spectra (XPS) of the samples were acquired on a VG Microtech Multilab ESCA 3000 with Al K_α radiation ($h\nu$ = 1486.6 eV). The peak corresponding to carbon 1s (at 285 eV) was taken as reference in estimating binding energy (BE) values of Au in the catalyst. The peak position was determined with a precision of ± 0.2 eV.

Reaction procedure

A known quantity of catalyst (0.05 g) and benzyl alcohol (25 mmol) were charged into a triple necked, glass, round-bottom flask (25 mL) placed in a temperature controlled oil bath. The reactor was connected with a water-cooled reflux condenser, a molecular oxygen/air-filled rubber balloon and a magnetic stirrer. Temperature of the reactor was raised to 80 - 120 °C and the reaction was conducted for a specific time. It was then cooled to 25 °C and

Journal Name

RSCPublishing

ARTICLE

Table 1 Chemical composition, textural properties and basicity of Au/ATNT catalysts

S. No.	Catalyst	Chemical composition (wt%)[a]			Textural properties[b]			Au particle/ crystallite size (d_{av}, nm)[c]	Au dispersion (%)[c]	Basicity (μmol/m^2)[d]		
		Au	Alkaline ion	Na^+	S_{BET} (m^2/g)	Pore volume (cc/g)	Pore diameter (nm)			Weak	Strong	Total
1	Au(1 wt.%)/LiTNT	0.62	2.21	0.92	178	0.56	5.1	11.6	10	0.46	0.80	1.26
2	Au(1 wt.%)/NaTNT	0.65	-	7.2	182	0.50	5.6	7.2	16	0.43	0.87	1.29
3	Au(1 wt.%)/KTNT	0.55	9.90	0.61	153	0.45	5.5	6.3	18	0.43	1.05	1.70
4	Au(3 wt.%)/KTNT	1.25	9.32	0.36	135	0.41	5.3	7.3[e]	-	0.40	1.13	1.53
5	Au(5 wt.%)/KTNT	3.33	8.80	0.22	122	0.38	5.1	15.4[e]	-	0.37	0.98	1.35
6	Au(1 wt.%)/CsTNT	0.52	16.42	2.6	126	0.32	4.1	10.0	11	0.45	1.72	2.17
7	Au(1wt.%)/MgTNT	0.90	2.50	0.62	165	0.41	5.6	9.9	12	0.21	2.12	2.19
8	Au(1 wt.%)/CaTNT	0.91	4.22	0.61	175	0.50	5.4	10.5 (10.0[e])	11	0.28	2.84	3.12
9	Au(1 wt.%)/SrTNT	0.72	9.21	0.30	173	0.44	5.5	5.4	19	0.25	2.82	2.75
10	Au(3 wt.%)/SrTNT	2.40	6.80	0.26	166	0.39	5.1	5.8[e]	-	0.36	1.9	2.26
11	Au(5 wt.%)/SrTNT	3.30	5.35	0.27	152	0.36	5.0	8.7[e]	-	0.41	1.78	2.19
12	Au(1 wt.%)/BaTNT	0.68	13.81	0.42	155	0.37	5.4	5.2	20	0.21	2.79	3.00
13	Au(3 wt.%)/BaTNT	2.80	12.00	0.36	146	0.36	5.3	5.5[e]	-	0.32	2.07	2.39
14	Au(5 wt.%)/BaTNT	4.10	9.26	0.28	140	0.35	5.1	6.4[e]	-	0.42	1.72	2.06
15	Au-Pd (1:1, 2 wt.%)/BaTNT	0.70 (0.82[f])	11.82	0.30	149	0.37	5.2	4.2	25	0.66	1.79	2.45

[a]ICP-OES. Alkaline ion means A^+ ion in ATNT. [b]N_2-physisorption. [c]HRTEM. [d]CO_2-TPD; weak (100 - 300 °C) and strong (300 - 500 °C). [e]Crystallite size from XRD. [f]Value in parentheses is the Pd content.

the catalyst was separated by centrifugation. For identification and quantification of products a GC–MS (Varian CP-3800; CP-Sil8CB — 30 m × 0.25 mm × 0.25 μm capillary column) and a gas chromatography (Varian 3800; CP-8907 — 15 m × 0.25 mm × 0.25 μm column and flame ionization detector) techniques were employed.

Results and discussion

Structural and textural characterization

NaTNT showed XRD peaks at 2θ = 10.1, 24.3, 28.4 and 48.5° corresponding to reflections from (200), (110), (211) and (020) planes, respectively (JCPDS files: 31-1329 and 41-0192). The ion-exchanged and Au loaded samples depicted similar XRD patterns indicating that they all have the same X-ray crystal structure as of NaTNT. The diffraction peak for (200) plane had, however, marginally shifted to a lower 2θ values (by 0.3°) when the cation in ATNT changed from Li^+ to Ba^{2+}. This shift in XRD peak position is due to increase in interplanar spacing with increasing size of the counterion. But the positions of other peaks remained nearly the same. Only representative XRD patterns of BaTNT and Au(1–3 wt%)/BaTNT are shown in Figure 1, while the patterns for all the other catalysts are deposited in supporting information (ESI†). No additional peaks due to Au were detected in 1 wt% Au deposited samples (except for Au/CaTNT) indicating that the size of Au particles in all those catalysts is below the detection limit of X-rays. However, at higher loading (ca., 3 and 5 wt%), additional peaks at 38.2° and 44.6° corresponding to Au(111) and Au(200) were observed (Figure 1). Further at high gold loadings, a decrease in the intensity of (200) [relative to (020)] was noted. This is due

to blockage of inter planar spacing with Au nanoparticles or structural deformation as a consequence of strong interaction of Au with the support titanate nanotubes.

HRTEM images and Au particle size distribution curves of Au(1 wt.%)/ATNT are shown in Figure 2. These images confirmed the presence of hollow tubular multi-walled morphology of the support titanate nanotube and the Au nanoparticles on the interior and outer surfaces of nanotubes. Metal dispersions (D) were determined using eqs. (1) and (2),

$$D = \frac{6V_m}{a_m d_{av}} \quad (1)$$

$$d_{av} = \frac{6\sum n_i V_i}{\sum n_i A_i} \quad (2)$$

where V_m = volume occupied by Au atom (1.69 x 10^{-23} cc), a_m = area occupied by Au atom (0.869 x 10^{-15} sq.cm), d_{av} = mean particle size of Au (HRTEM), V_i = volume of i^{th} particle (HRTEM) and A_i = surface area of i^{th} particle (HRTEM). Mean particle size and percentage dispersion of Au estimated from HRTEM images are listed in Table 1. Wherever the characteristic peaks due to Au were observed in XRD, average crystallite size of Au was determined using the Debye-Scherrer formula and reported in Table 1. The crystallite (XRD) and particle sizes (HRTEM) of Au(1 wt%)/CaTNT are comparable. The value of d_{av} for different Au(1 wt%)/ATNT is in the range 5.2 – 11.6 nm and Au dispersion is between 10 and 20%.

Chemical composition (Au, alkali/alkaline earth metal ion and Na^+ contents) of Au/ATNT catalysts was determined by ICP-OES (Table 1). The Na/Ti mole ratio of "bare" NaTNT was 0.65, which is nearly equal to the theoretical value of 0.67 confirming the molecular formula of NaTNT as $Na_2Ti_3O_7$. Ion-exchange with other alkali/alkaline earth metal ions occurs along the length of the nanotube. Na^+ ions in interlayer region were difficult to exchange and hence, reminiscence of non-exchangeable Na^+ may be noted in the compositions of Au/ATNT (Table 1).

Representative N_2 adsorption-desorption isotherms along with pore size distribution curves of BaTNT and Au(1 wt%)/BaTNT are shown in Figure 3. These materials showed N_2 physisorption isotherms typical of type IV with H_2-hysteresis loop. The isotherms represent mesoporosity with open-ended pore structure. The samples showed broad pore size distribution curves. Size of the alkali/alkaline earth metal ion has an influence on the textural properties. S_{BET} of Au/ATNT was in the range 122 – 182 m^2/g and average pore diameter was between 4.1 and 5.6 nm (Table 1). Bare supports have S_{BET} between 132 and 196 m^2/g and average pore diameter between 4.5 and 6.6 nm (ESI†). A marginal decrease in specific surface area and average pore diameter is thus noted upon loading Au. A decrease in total pore volume of Au/ATNT compared to the supports was also observed.

Carbon dioxide was used as a probe molecule to determine the basicity of Au/ATNT catalysts. The TPD profiles (ESI†) contained two desorption peaks, in the temperature regions 100–300 °C and 300–500 °C corresponding to weak and strong basic sites, respectively. Desorption temperature and the amount of CO_2 desorbed refer to the strength and density of basic sites. Basicity of the catalysts is reported in Table 1. In general, the alkaline earth metal ion exchanged titanates have higher basicity than the alkali metal ion exchanged catalysts. It appears that the amount of ions exchanged also determined the basicity value. Basicity of the catalysts influenced the uptake and particle size of Au (ESI†). Au(1 wt%)/NaTNT showed an additional weak overlapping peak at 250 – 300 °C which is rather missing in other ATNT samples.

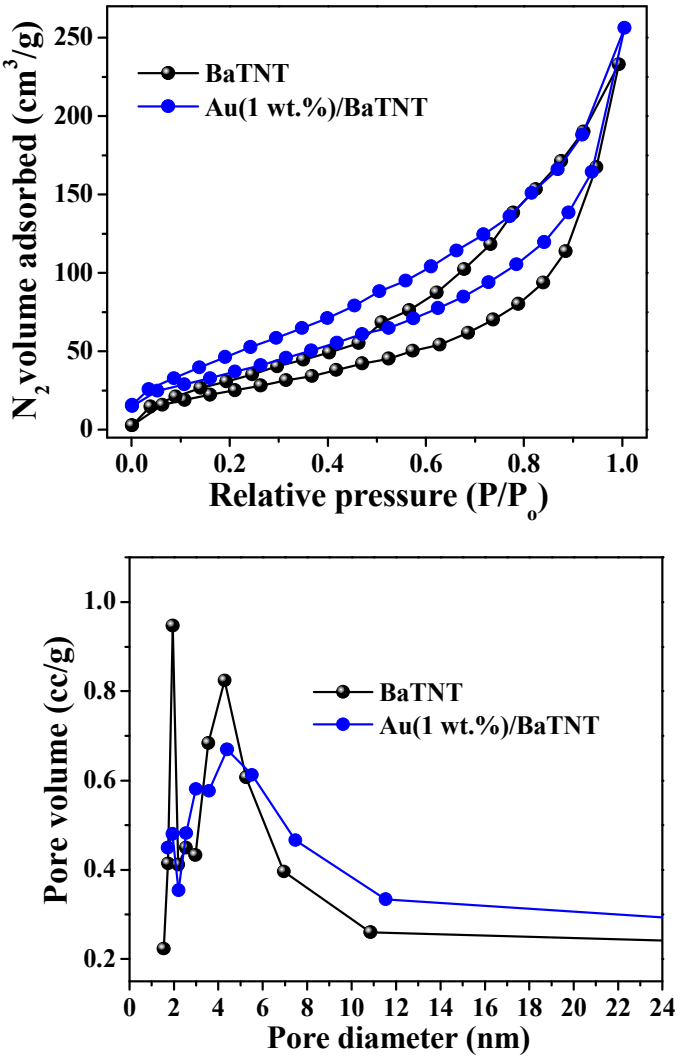

Figure 3 N_2-physisorption isotherms (top) and pore size distribution curves (bottom) of BaTNT and Au(1 wt.%)/BaTNT.

Among alkali ion exchanged Au/ATNT catalysts the uptake of Au (Au content in the catalyst) decreased with increasing basicity of the catalyst. Similar observation was found also for alkaline earth metal ion exchanged Au/ATNT catalysts. In general, the percentage Au uptake (with respect to the input value) is higher for alkaline earth metal ion than alkali ion exchanged ATNT. Also a decrease in the mean size (d_{av}) of Au with increasing basicity of the catalyst was observed (ESI†) with the values of Au supported on Cs^+, Mg^{2+} and Ca^{2+}-exchanged NaTNT deviating from this relationship. Reason for this abnormal behaviour is not clear at this point of time. However, it appears that strength of basicity and relative concentration of strong basic sites may influence the metal particle size.

Spectral Characterization

DRUV–vis spectroscopy provided evidence for the presence of Au nanoparticles by showing a typical localized surface

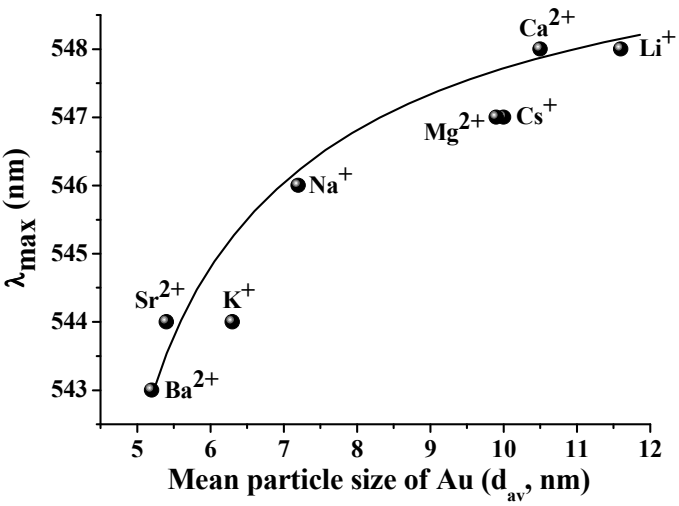

Figure 4. Variation of LSPR band position (λ_{max}) with the mean particle size (d_{av}) of supported Au.

plasmon resonance (LSPR) band at 480-580 nm (ESI†). The peak position of LSPR band (λ_{max}) is related to the Au mean particle size. It is related to the shape of Au particle and dielectric function of the support material. As seen from Figure 4, λ_{max} of LSPR band increased with increasing particle size of Au. We have already noted that the particle of Au has an inverse relation with the basicity of the catalyst. In other words, the spectral/electronic properties of Au are greatly influenced by the nature of the support and Au particle size. Similar observations were made also by other researchers[22].

Au(1 wt%) supported on KTNT, SrTNT and BaTNT showed $4f_{7/2}$ line in XPS at 83.2, 83.0 and 82.8 eV, respectively, Metallic gold in gold foil shows this line at 84.0 eV.[23] This suggests that Au on ATNT is rich in electron density. The formation of such electron rich Au species was attributed to occur through transfer of the electron density from the support[23, 24]. Arrii et al.[25] have reported the dependence of Au $4f_{7/2}$ binding energy on the nature of the support. On TiO_2 and Al_2O_3, BE of Au $4f_{7/2}$ showed a negative shift by −0.6 and −0.9 eV, respectively. A large shift up to −1.1 eV was observed for the spent Au/TiO_2 catalyst. When the cations were changed from K^+ to Sr^{2+} and Ba^{2+} in ATNT, the BE of Au signals shifted systematically downward (Table 2). This observation indicates that as the basicity of the support increased, the Fermi level of the metal particles shifted to a lower binding energy. Thus, the XPS points out electron transfer from ATNT to Au nanoparticles, the extent of which follows the order: BaTNT > SrTNT > KTNT. Deconvolution of the XPS lines in the Au binding energy region (ESI†) revealed the presence of another set of signals at higher BE values but with lower intensity assignable to $Au^{\delta+}$ ions. Pusztai et al[23] reported that, on titanate nanowires, gold atoms can occupy ion exchange positions at lower loading. They observed a higher portion of Au^+/Au^0 on the catalyst after reduction with H_2 compared to reduction with $NaBH_4$. This may be a reason for the presence of a small quantity of $Au^{\delta+}$ species in ATNT samples. There are reports[26, 27], which argue that hydride transfer is involved in C–H bond activation, and the cationic gold is catalytically active. Abad et al.[27] have investigated the active sites on Au/CeO_2. Recently, Zhao et al.[28] have also reported the active sites on Au/Ni_2O_3 involved in oxidation of alcohol. They showed a direct

Table 2 XPS data (binding energy values in eV) of Au/ATNT catalysts

Catalyst	$\frac{Au^{\delta+}}{Au^0}$	Au^0		$Au^{\delta+}$	
		$4f_{7/2}$	$4f_{5/2}$	$4f_{7/2}$	$4f_{5/2}$
Au(1 wt.%)/KTNT	0.28	83.2	86.9	85.2	88.9
Au(1 wt.%)/SrTNT	0.27	83.0	86.7	85.2	88.9
Au(1 wt.%)/BaTNT	0.43	82.8	86.5	85.3	89.0
Au-Pd(1:1, 2 wt.%)/BaTNT	-	82.7	-	85.4	-

correlation between the concentration of Au^+ or Au^0 species and catalyst supports. Au^+/Au^0 ratio in the present catalysts was determined (Table 2). Lower the BE value higher was the catalytic activity over Au/ATNT catalysts (ESI†). For Au–Pd(2 wt.%, 1:1)/BaTNT, the core level XPS for Au $4f_{7/2}$ line appeared at 82.7 eV (ESI†). Weak intensity of these Au 4f lines is indicative of the location of Au inside the titanate nanotubes and masking of Au surface by Pd particles. Smaller particle size can also lead to lowering in BE values. The spectral lines for Pd^0 appeared at 334.8 eV ($3d_{5/2}$) and 340.0 eV ($3d_{3/2}$).

Catalytic activity

The catalytic activity of Au supported on ATNT for benzyl alcohol oxidation with molecular oxygen as oxidant was studied at 120 °C and under solvent- and alkali-free conditions (Table 3). Benzaldehyde was the selective product (selectivity = 99 wt.%). While the support has little effect on benzaldehyde selectivity, a remarkable influence of it on benzyl alcohol conversion and turnover frequency (TOF) was observed (Table 3). Au(1 wt.%) supported on Ba^{2+} ion-exchanged NaTNT [Au(1 wt.%)/BaTNT] showed highest catalytic activity [benzyl alcohol conversion = 43 wt.% and TOF = 622 h^{-1} (based on total metal content) and 2237 h^{-1} (based on exposed surface metal atoms)]. This reaction occurred also with air instead of molecular oxygen over Au(1 wt.%)/BaTNT but then the conversion under same reaction conditions was 24.6 wt.% with benzaldehyde selectivity of 96.5 wt.%. Support (BaTNT) alone could not catalyze this reaction to a notable extent (benzyl alcohol conversion = 2.8 wt.%). The gold nanoparticles were smaller in size (d_{av} = 5.2 nm) and highly dispersed (metal dispersion = 20%) on BaTNT than on other supports (Table 1). Smaller the particle size, higher would be the number of exposed surface active sites and interaction with the support and higher would be the catalytic activity. The catalytic activity of Au(1 wt.%) supported on KTNT, SrTNT and BaTNT with almost similar Au particle size followed the order: Au(1 wt.%)/BaTNT > Au(1 wt.%)/SrTNT > Au(1 wt.%)/KTNT (Table 3, run nos. 3, 9 and 12a). This trend in catalytic activity parallels the variation in electron transfer from support to Au particles. With a view to see the influence of addition of Pd on the catalytic activity of Au, we have prepared a Au-Pd (2 wt%, 1:1)/BaTNT composition. Addition of Pd decreased the mean particle size of Au from 5.2 to 4.2 nm and metal dispersion increased from 20 to 25%. Au-Pd/BaTNT showed remarkably high catalytic activity than the catalyst without Pd content (benzyl alcohol conversion = 92.3 wt.% as against 43 wt%). But the benzaldehyde selectivity dropped from 99 to 80.5 wt.%. Note that 92.3% conversion on Au-Pd was achieved in just 5 h instead of 10 h. Hence, Au supported on NaTNT exchanged with larger cations exhibited higher catalytic activity due to higher amount of e^- density at Au in those catalysts, which could easily activate molecular oxygen and enable the oxidation

Table 3 Catalytic activity data for oxidation of benzyl alcohol over Au/ATNT catalysts[a]

Run no.	Catalyst	Conversion (wt.%)	TOF (h^{-1})	Aldehyde selectivity (wt.%)b
1	Au(1 wt.%)/LiTNT	7.2	114 (852)	99.0
2	Au(1 wt.%)/NaTNT	17.0	257 (1153)	99.0
3	Au(1 wt.%)/KTNT	21.9	392 (1583)	99.0
4	Au(3 wt.%)/KTNT	34.1	268	98.2
5	Au(5 wt.%)/KTNT	45.3	134	93.6
6	Au(1 wt.%)/CsTNT	8.8	166 (1068)	99.0
7	Au(1 wt.%)/MgTNT	11.6	127 (805)	99.0
8	Au(1 wt.%)/CaTNT	13.4	147 (976)	99.0
9	Au(1 wt.%)/SrTNT	37.8	516 (1791)	99.0
10	Au(3 wt.%)/SrTNT	46.3	190	96.2
11	Au(5 wt.%)/SrTNT	54.1	161	94.1
12a	Au(1 wt.%)/BaTNT	43.0	622 (2237)	99.0
12b	Au(1 wt.%)/BaTNT	24.6	356 (1280)	96.5
13	Au(3 wt.%)/BaTNT	62.5	220	97.0
14	Au(5 wt.%)/BaTNT	69.7	167	95.2
15	Au-Pd(1:1, 2 wt.%)/BaTNT	92.3	819 (4653)	80.5

[a]Reaction conditions: catalyst = 0.05 g, benzyl alcohol = 25 mmol, $p(O_2)$ = 1 atm, reaction temperature = 120 °C, and reaction time = 10 h, Turnover frequency (TOF) = moles of benzyl alcohol converted per mole of Au in the catalyst (ICP-OES) per hour.TOF values in parentheses are those calculated based on mole of benzyl alcohol converted per mole of surface metal atoms (estimated from HRTEM) per hour. Run no. 12a is performed with molecular oxygen. Run no. 12b was conducted with air. For run no. 15, reaction time = 5 h and the product includes benzaldehyde (80.5%), benzoic acid (1.0%), benzyl benzoate (10.2%), benzene (6.2%) and toluene (2.1%). [b]Balance selectivity is benzyl benzoate.

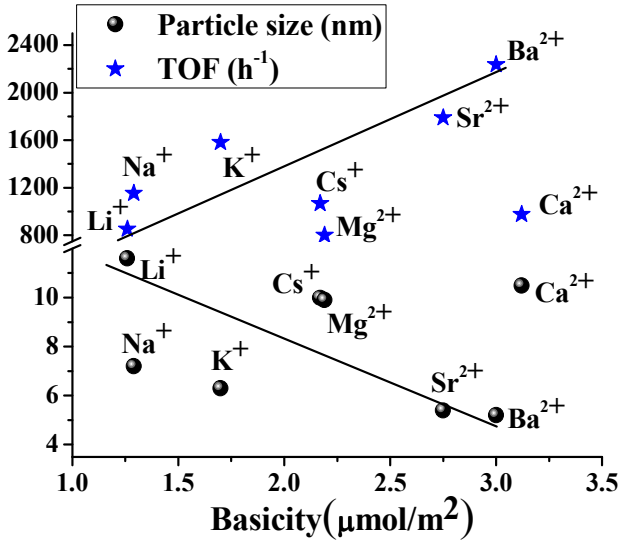

Figure 5. Variation of mean particle size and TOF with the basicity for Au(1 wt.%)/ATNT. Reaction conditions: catalyst = 0.05 g, benzyl alcohol = 25 mmol, $p(O_2)$ = 1 atm, reaction temperature = 120 °C, and reaction time = 10 h.

of benzyl alcohol.[29] Hsu et al[14] observed such electronic effect on Pt catalysts with similar supports. Figure 5 shows an interesting correlation between basicity and mean particle size / catalytic activity (TOF). Particle size of Au decreased with increasing basicity (basic sites per unit surface area) of the catalyst while TOF showed an increasing trend. In other words,

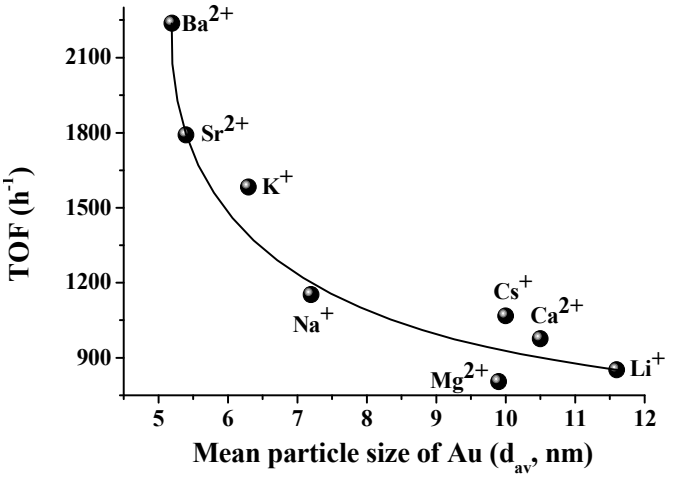

Figure 6 Correlation between turnover frequency (TOF) and mean particle size of Au. Reaction conditions same as in Figure 5.

basicity of the support, mean particle size of Au and catalytic activity are inter-related to each other. The points related to Au(1 wt%) on CaTNT and MgTNT have fallen away from this relationship because there could be other factors like strength of basicity that would influence the values of particle size and TOF. Figure 6 depicts the variation of oxidation activity of Au as a function of its particle size. Catalytic activity increased with decreasing Au particle size. It is interesting to note that all the catalysts have followed this trend unlike that observed in Figure 5. This clarifies that other than density, strength of basicity plays a crucial role. With increasing Au content from 1 to 5 wt.% on BaTNT, the conversion of benzyl alcohol increased from 43 to 69.7 wt.% but the selectivity for benzaldehyde decreased from 99 to 95.2 wt.% (Table 3). Increase in activity with increasing Au content was observed also with KTNT and SrTNT supports.

Effect of the reaction conditions

Catalytic activity increased with increasing reaction time (ESI†). Only a marginal drop in benzaldehyde selectivity was noted at higher conversions. Also an increase in activity with the amount of the catalyst was noted (ESI†). When the reaction temperature was raised from 80 to 100 and then to 120 °C, benzyl alcohol conversion on Au(1 wt.%)/BaTNT increased from 30.2 to 36.3 and then to 43 wt.%. This increase was from 8.4 to 15.2 and then to 17 wt.% over Au(1 wt.%)/NaTNT. Selectivity for benzaldehyde was 99 wt.% at all those conditions (ESI†).

Catalyst reusability

Figure 7 displays reusability of Au(1 wt.%)/BaTNT in benzyl alcohol oxidation. After the first run, the catalyst was separated from the reaction mixture by filtration, washed with water, dried at 110 °C for 4 h and then, reused in the next recycle conducted at the same conditions. Such recycles were done for five times. The catalyst was recyclable. The XRD of the spent catalyst is nearly the same as that of the fresh one (Figure 1). ICP-OES analysis of spent catalyst showed no loss of Au content but a little loss of Ba^{2+} ion (0.6 wt%) at the end of 5th recycle was detected. To confirm the heterogeneity of oxidation

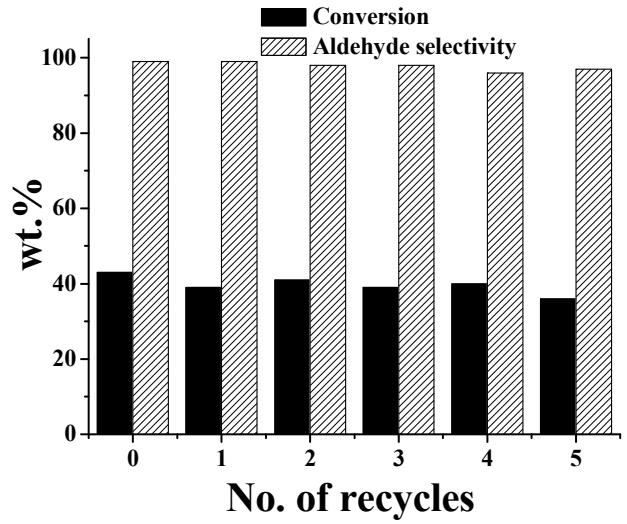

Figure 7 Recyclability of Au(1 wt%)/BaTNT in the oxidation of benzyl alcohol with molecular oxygen. Reaction conditions same as in for Figure 5.

reaction over Au(1 wt.%)/BaTNT, the reaction at 120 °C was stopped after 2 h (when the conversion was 17.2 wt.%), catalyst was taken out and the reaction was continued without the catalyst for another 8 h and the reaction mixture was analyzed by GC. No detectable change in benzyl alcohol conversion was observed (ESI†) suggesting that the reaction was heterogeneous in nature.

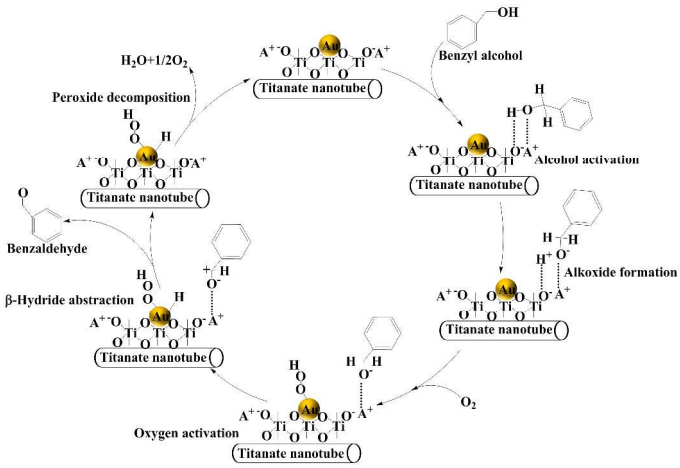

Figure 8. Tentative mechanism for the oxidation of benzyl alcohol over Au/ATNT.

Electrooxidation of ethanol over Au supported on glassy carbon requires a partial coverage of Au surface with its oxide species. In CO oxidation, it was found that the oxidation activity increases with increase in the concentration of Au^+ species; but the presence of metallic Au (electron rich) was essential. According to these reports, the active sites consist of an ensemble of metallic Au atoms and a cationic Au^+ species.[30-32] In the present case, benzyl alcohol is activated on the support surface (as a consequence of its basic nature). Then the abstraction of hydride ion is favoured at the metal-support interface (at coordinatively unsaturated sites/Au^+ ions). The electron rich Au nanoparticles activate molecular oxygen to produce activated oxygen species, which help removing H from AuH species to produce water as by-product. Meanwhile, the benzyloxy cation releases proton and forms the final product benzaldehyde.[33, 34] A schematic representation of reaction mechanism is shown in Figure 8. Particle size of Au decreased with increasing basicity of the support while the catalytic activity had increased (Figure 5). Higher the basicity higher would be the activation of benzyl alcohol and more would be the conversion. At the same time, lower the particle size of Au, higher would be the available surface area and support-Au interaction and higher would be activation of molecular oxygen and thereby, higher would be the catalytic activity. Thus, basicity has a direct (by way of activating benzyl alcohol) and indirect (by way of support-metal interaction) influence on the catalytic activity. The mean particle size of Au on different supports decreased in the order: Au/BaTNT < Au/SrTNT < Au/KTNT. Smaller the particle size higher would be the SMSI effect, more would be the peripheral Au that are in δ+ state and hence, higher would be the hydride ion abstraction and thereby, higher would be the catalytic activity. This behavior is clearly evident from the XPS and catalytic activity data.

Conclusions

Gold supported on alkali and alkaline earth metal ion-exchanged titanate nanotubes (ATNT) were synthesized, characterized and their catalytic activities for benzyl alcohol oxidation with molecular oxygen/air were investigated. Gold particles on ATNT have a mean diameter in the range of 5.2 – 11.6 nm and Au dispersion in the range of 10 - 20%. Oxidation of benzyl alcohol formed benzaldehyde with a selectivity of 99 wt.%. Alkali and alkaline metal ion exchange has a marked effect on the catalytic activity of titanate nanotubes. Among the catalysts investigated Au supported on BaTNT showed highest catalytic activity. Basicity of the support has an influence on the mean particle size and catalytic activity of Au. With increasing basicity, the particle size of Au has decreased while the activity of the catalyst has increased. This study teaches that catalytic activity of Au can be enhanced by altering the titanate support through exchanging with Ba^{2+} ions. Since Au draws electron density from the basic support, it can activate molecular oxygen more easily forming superoxide like active oxygen species which in turn initiate the oxidation reaction.

Acknowledgements

D. N. acknowledges the Council of Scientific and Industrial Research (CSIR), New Delhi, for the award of Senior Research Fellowship.

Notes and references

[a] Catalysis Division, CSIR-National Chemical Laboratory, Pune 411 008, India. Fax: +91 20 2590 2633; Tel: +91 20 2590 2018; E-mail: d.srinivas@ncl.res.in.
[b] Academy of Scientific and Innovative Research (AcSIR), New Delhi 110 001, India.

Electronic Supplementary Information (ESI) available: [XRD, CO_2-TPD profiles, DRUV-vis spectra and XPS profiles of Au/ATNT, N_2 physisorption of supports, correlation profiles of basicity verses uptake and particle size of Au and B.E. values versus TOF and catalytic activity data]. See DOI: 10.1039/x0xx00000x/

1 G. J. Hutchings, J. Catal., 1985, 96, 292.
2 M. Haruta, T. Kobayashi, H. Sano and N. Yamada, Chem. Lett., 1987, 16, 405.
3 Y. Zhang, X. Cui, F. Shi and Y. Deng, Chem. Rev., 2012, 112, 2467.
4 C. D. Pina, E. Falletta and M. Rossi, Chem. Soc. Rev., 2012, 41, 350.

5 S. J. Tauster, S. C. Fung, R. L. Garten, J. Am. Chem. Soc., 1978, 100,170.
6 V. E. Herinch and P. A. Cox, The Surface Science of Metal, Cambridge University Press, Cambridge, 1996.
7 A. Bruix, J. A. Rodriguez, P. J. Ram rez, S. D. Senanayake, J. Evans, J. B. Park, D. Stacchiola, P. Liu, J. Hrbek and F. Illas, J. Am. Chem. Soc., 2012, 134, 8968.
8 C. T. Campbell, Nat. Chem., 2012, 4, 597.
9 M. Valden, X. Lai and D.W. Goodman, Science, 1998, 281, 1647.
10 J. K. Nørskov, T. Bligaard, B. Hvolbæk, F. Abild-Pedersen, I. Chorkendorff and C. H. Christensen, Chem. Soc. Rev., 2008, 37, 2163.
11 C. Milone, R. Ingoglia, A. Pistone, G. Neri and S. Galvagno, Catal. Lett., 2003, 87, 201.
12 T. Kasuga, M. Hiramatsu, A. Hoson, T. Sekino and K. Niihara, Langmuir, 1998, 14, 3160.
13 X. Sun and Y. Li, Chem. Eur. J., 2003, 9, 2229.
14 C. Y. Hsu, T. C. Chiu, M. H. Shih, W. J. Tsai, W. Y. Chen and C. H. Lin, J. Phys. Chem. C, 2010, 114, 4502.
15 M. Hodos, Z. Kónya, G. Tasi and I. Kiricsi, React. Kinet. Catal. Lett., 2005, 84, 341.
16 M. A. Khan and O. B. Yang, Catal. Today, 2009, 146, 177.
17 V. Idakiev, Z. Yuan, T. Tabakova and B. Su, Appl. Catal. A: Gen., 2005, 281, 149.
18 L. C. Sikuvhihulu, N. J. Coville, T. Ntho and M. S. Scurrell, Catal. Lett., 2008, 123, 193.
19 T. A. Ntho, J. A. Anderson and M. S. Scurrell, J. Catal., 2009, 261, 94.
20 L. T. Murciano, Q. He, G. J. Hutchings, C. J. Kiely and D. Chadwick, ChemCatChem, 2014, 6, 2531.
21 D. Nepak and D. Srinivas, Catal. Comm., 2015, 58, 149.
22 P. Claus, A. Bruckner, C. Mohr and H. Hofmeister, J. Am. Chem. Soc., 2000, 122, 11430.
23 P. Pusztai, R. Puskas, E. Varga, A. Erdohelyi, A. Kukovecz, Z. Konyaad and J. Kiss, Phys. Chem. Chem. Phys., 2014, 16, 26786.
24 J. Y. Tsai, J. H. Chao and C. H. Lina, J. Mol. Catal. A: Chem., 2009, 298, 115.
25 S. Arrii, F. Morfin, A. J. Renouprez, and J. L. Rousset, J. Am. Chem. Soc., 2004, 126, 1199.
26 M. Wang, F. Wang, J. Ma, M. Li, Z. Zhang, Y. Wang, X. Zhang and J. Xu, Chem. Commun., 2014, 50, 292.
27 A. Abad, P. Conception, A. Corma and H. Garcia, Angew. Chem. Int. Ed., 2005, 44, 4066.
28 G. Zhao, J. Huang, Z. Jiang, S. Zhang, L. Chen and Y. Lu, Appl. Catal., B: Env., 2013, 140–141, 249.
29 C. Santra, S. Rahman, S. Bojja, O. O. James, D. Sen, S. Maity, A. K. Mohanty, S. Mazumder and B. Chowdhury, Catal. Sci. Technol., 2013, 3, 360.
30 G. C. Bond and D. T. Thompson, Gold Bull., 2000, 33, 41.
31 T. Mallat and A. Baiker, Chem. Rev., 2004, 104, 3037.
32 M. S. Chen and D. W. Goodman, Catal. Today, 2006, 111, 22.
33 H. Liu, Y. Liu, Y. Li, Z. Tang and H. Jiang, J. Phys. Chem. C, 2010, 114, 13362.
34 X. Zhang, X. Ke and H. Zhu, Chem. Eur. J., 2012, 18, 8048.